

# Strain-induced crystallisation in bulk amorphous PET under uni-axial loading

E. Gorlier, J.M. Haudin, N. Billon\*

*Ecole des Mines de Paris, CEMEF, UMR CNRS 7635, BP 207, 06904 Sophia-Antipolis Cedex, France*

Received 18 April 2001; received in revised form 22 April 2001; accepted 29 June 2001

## Abstract

Strain induced crystallisation of poly(ethylene terephthalate) (PET) designed for stretch-blow moulding is studied combining well-controlled tensile tests, different quenching protocols and X-ray diffraction technique. As well known [Polymer, 33 (1992) 3182; Polymer, 33 (1992) 3189], crystallisation begins when a minimum strain has been reached. However, crystallisation is a progressive phenomenon that could involve intermediate stages or phases as suggested by some recent papers [Macromolecules, 31 (1998) 7562; Polymer, 41 (2000) 1217]. In this study, first evidence for the crystallisation is the appearance, parallel to the tensile direction, of zones having the crystal lateral order. The spreading out of the diffraction dots suggests that these zones are small in comparison to usual lamella thickness or that the order is imperfect. Longitudinal order appears later, progressively leading to fibre-texture. At low strain, before this texture is totally developed, cooling influences the final microstructure superposing steps in which crystallisation and relaxation compete illustrating the relative importance of cooling protocol when strain induced crystallisation of PET is studied. Nevertheless, strain hardening can be observed before the crystalline microstructure is totally developed, emphasising the fact that strain hardening is mainly controlled by first stages of crystallisation and that actual crystallisation occur during a following relaxation step. © 2001 Elsevier Science Ltd. All rights reserved.

*Keywords:* PET; Crystallisation; Strain hardening

## 1. Introduction

Because of its slow crystallisation kinetics, molten Poly(ethylene terephthalate) (PET) can be cooled down either to a quasi-fully amorphous or to a semi-crystalline state depending on the cooling rate. Once it has been quenched into its amorphous state, PET can further crystallise under strain in its rubber-like state (i.e. above its glass transition temperature). Induced microstructure is then specific (e.g. small oriented crystals) and leads to properties different from those of the same PET crystallised from the melt.

This ability of PET to develop a specific semi-crystalline microstructure under mechanical loading above glass transition is the basis of important applications such as film bi-orientation, fibre spinning and stretch-blow moulding. In such cases, PET is first obtained as an amorphous half-finished product (e.g. a preform in the case of stretch-blow moulding) to be further deformed. Prior to this final processing, the parts are heated above the glass transition (i.e. from 90 to 110°C) and below the crystallisation temperature (e.g. below 120°C). Processing itself consists

of a tight combination of rapid and more or less complex mechanical loading conditions (uni-axial or multi-axial) and cooling kinetics, sometimes completed with thermal treatments. Whatever the process is, local deformation history is neither simple nor intuitive, and strain-rates as well as induced strains are generally high.

Final properties of the material strongly depend on the induced microstructure which, for its part, depends on and, to some extent, controls this complex thermo-mechanical history. As a consequence, it is of prime interest to observe and to understand the development of the crystalline phase as a function of loading conditions. Due to the complexity of industrial processes, this has been intensively studied in more simple conditions reproducing one or more of the various processing steps: deformation at constant load or velocity; uni- or bi-axial loading; thermal treatments under constant load or deformation.

Despite this abundant literature, knowledge of the microstructure development in PET remains insufficient when one aims at models for final properties prediction. As a matter of fact, some uncertainties remain concerning the actual crystallisation kinetics under strain and the way crystallisation can be accounted for in constitutive models in processing modelling. Additionally, most of the previous

\* Corresponding author. Tel.: +33-4-93957420; fax: +33-4-92389752.  
E-mail address: noelle.billon@cemef.cma.fr (N. Billon).

studies were performed on fibres or films. Consequently, it would be interesting to know to what extent previous observations could be extrapolated to stretch-blow moulding, which involves thick samples.

This represents the general goal of the study of this paper to propose a possible scheme for the development of the microstructure during stretch-blow moulding of PET. As a first step, simple uni-axial loading conditions and thick samples are used to lead to unambiguous results and to be representative for preforms, respectively. X-ray diffraction patterns are performed as a function of strain during tensile tests conducted under conditions as controlled as possible. Results are analysed in a qualitative way to estimate the moment when crystallisation is effective. Mechanical tests are performed under isothermal conditions and at constant strain-rate. As X-ray diffraction experiments are not on-line measurements, the effect of the quenching protocol after the mechanical tests is also considered. Finally, present experiments are discussed accounting for, and enlightening some of, the well-admitted and more recent results of the literature on this topic.

## 2. Bibliography review: kinetics of strain-induced microstructure development in PET

Microstructure development in PET has been extensively studied combining different techniques such as Infra-Red, Raman and fluorescence spectroscopies, X-ray diffraction, birefringence and density measurements on thin samples. An exhaustive list of relevant papers should be too long in this context. However, some main points have to be emphasised.

It seems now well admitted that deformation of PET above glass transition leads to:

- a decrease in the amount of glycol groups exhibiting a gauche conformation, due to chain extension [1],
- a progressive tip over of the aromatic cycles parallel to the plane of the deformation [1–5],
- the development of a highly oriented amorphous phase consisting of chains in their *trans* conformation whereas gauche conformers are confined in a less oriented amorphous phase [1,6–8],
- the appearance of small and oriented crystals [9,10] involving only chains having a *trans* configuration [1].

Whatever the loading conditions are (constant load [13], velocity [11] or strain-rate [14]), a minimum stretching, depending on strain-rate and temperature, appears to be necessary to promote a significant amount of crystalline phase. Crystallinity ratio vs draw ratio is an S-shaped curve [8,11,12] as crystallinity is almost negligible up to draw ratios of 2–2.5 and then increases up to value of 33% for draw ratios ranging from 4 to 5. As far as mechanical properties are concerned, this crystallisation is

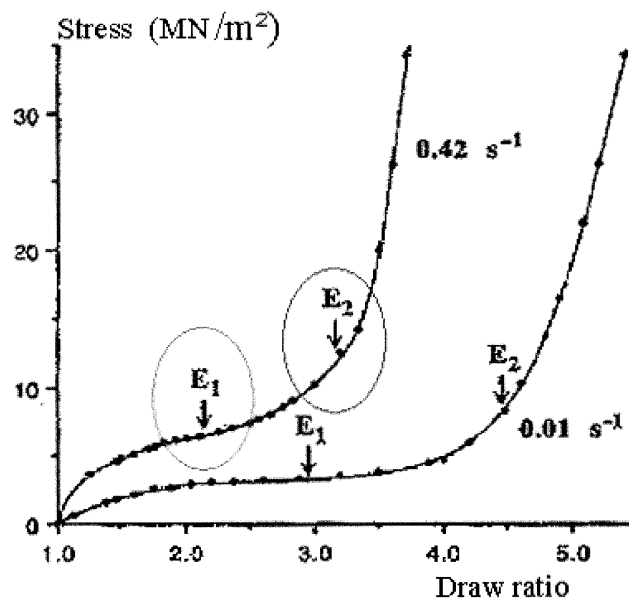


Fig. 1. True stress vs draw ratio at two strain rates. The onset of crystallisation, E1, and the onset of regime 2 crystallisation, E2, are indicated [15].

associated with a spectacular strain hardening. According to Salem [15,16] and based on density measurements, the deformation can be decomposed into two stages (Fig. 1): a first step combining a smooth increase of the stress and a rapid crystallisation (up to 15% crystallinity) and a final step combining a drastic increase in the stress and an almost constant crystallinity ratio.

All these observations are generally not in-situ measurements and require an intermediate cooling down of the sample. It means that between the deformation and the measurement, the material has to be quenched. In such a situation, the induced crystalline phase always consists of oriented microfibrils [17–25] embedded in a more or less oriented amorphous phase. However, three facts have to be emphasised at this point:

- First, crystallisation kinetics of PET is drastically increased by molecular orientation. As an example, crystallisation time, usually ranging from a few seconds to a few minutes (depending on the temperature), can decrease down to 100 to 1 ms if PET is oriented [17,26].
- Second and consequently, the global strain-induced microstructure remains sensitive to further thermal treatments. The reported modifications during annealing result from a competition between molecular relaxation, epitaxial transverse growth and lamellae thickening [17–19,27,28], orientation remaining often important.
- Thirdly, it is almost impossible to instantaneously cool down a polymer.

As a consequence, one can argue that, depending on the experimental protocol for quenching that is not often well described in papers, the material may remain at a temperature

higher than that of the glass transition during a certain time after deformation. As a matter of fact, taking into account the crystallisation times in oriented PET [17,26] and the efficiency of usual thermal treatments, observations made after cooling could then result from both the deformation and a post-crystallisation occurring during freezing.

Recently, on-line observations at high strain-rates, using synchrotron X-ray beam, suggesting that crystallisation could not occur during deformation have been reported [29,30]. Even if these results have to be considered with caution, as characteristic times of the techniques should also be accounted for, one can imagine that the exact crystallisation kinetics may not be totally accessible through usual protocols.

Additionally, strain-induced crystallisation should be a more progressive process than suggested by Salem. Some authors report the existence of a smectic phase in the earlier stages of crystallisation, acting as precursor and disappearing to form an imperfect crystal or mesophase which develops by becoming more and more ordered [31,33].

### 3. Material and protocol

#### 3.1. Material

A PET designed for stretch-blow moulding application whose average molar mass  $M_n$  is  $19,000 \text{ g mol}^{-1}$  and that is supplied by Tergal Fibres is chosen. This type of PET is slightly different from those used in previous study in connection with film or fibre applications. As a matter of fact, crystallisation kinetics is slowed down due to a few percent of isophthalic acid (IPA) and diethylene glycol (DEG) [34,35].

The glass transition temperature of this material is found to be equal to 77 and 82°C using DSC (Differential Scanning Calorimetry) analysis at a cooling rate of  $10^\circ\text{C min}^{-1}$  and DMTA (Dynamical Mechanical and Thermal Analysis) measurements at  $1 \text{ rd s}^{-1}$  and for a heating rate of  $1^\circ\text{C min}^{-1}$ , respectively. Crystallisation in the rubber state and under quiescent conditions occurs, for its part, at temperatures ranging from 110 to 120°C.

Thick 4 mm-diameter hourglass-shaped (Fig. 2) samples are injection moulded in such a way that the material remains amorphous and that its intrinsic viscosity does not vary, i.e. after a drying ensuring less than 50 ppm of residual water in the granules. This protocol makes the samples representative for thick preforms. The absence of crystallinity is checked through X-ray diffraction patterns. The fact that intrinsic viscosity does not vary during processing makes it possible to conclude that the average molar mass remains constant. Samples are used a few weeks after processing without any additional drying, but under stable water conditions.

#### 3.2. Tensile tests

A video-controlled system [36] coupled with specific clamping devices is used. This system makes it possible to determine the actual diameter of the sample in its necking zone as a function of time and to control the crosshead velocity to ensure that the strain-rate remains locally constant. Unfortunately, despite the initial shape of the sample, once necking is developed and due to the drastic strain hardening process in PET, an important deformation of the shoulders of the specimen is observed during isothermal measurements. Consequently, these experiments should be restricted to low deformation without specific devices. As a matter of fact, to reach high-strain levels (i.e. 2.5) shoulders have to be cooled down below glass transition to remain rigid. Obviously, in such a case, temperature in the specimen is no more homogeneous. However, thanks to the video-controlled system, the only temperature to be controlled is the temperature of the central zone of the sample (i.e. the zone where the system controls strain-rate). Specific cooled clamping devices are then used together with a specific protocol consisting of cooling the shoulders as late as possible to keep the temperature of the central zone of the specimen constant throughout the entire tests without deforming the shoulders. This protocol is defined using calibration tests with thermocouples embedded in samples and finite element calculations.

Sets of experimental conditions (temperature and strain-rate) are chosen among those for which PET exhibits a behaviour qualitatively equivalent to that it exhibits during processing (i.e. rubber-like behaviour), but ensuring that the experiments remain feasible: i.e. from 85 to 105°C and from 0.001 to  $0.01 \text{ s}^{-1}$ . An additional choice criterion is the absence of significant quiescent crystallisation during the test, i.e. the temperature and the duration of the experiments (including heating time as the samples are massive) have to be adjusted for static crystallisation to remain negligible. This is done on the basis of DSC analysis of the crystallisation kinetics.

To conclude, our protocol allows us to determine true stress vs true strain curves at constant true strain-rate and constant temperature up to high strain [37–39] for a PET in its rubber-like state and ensuring that the only crystallisation

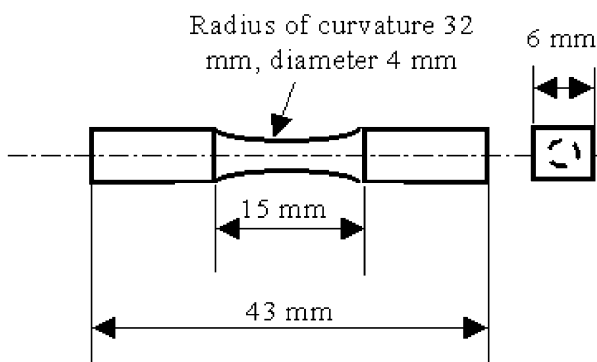


Fig. 2. Dimensions of the hourglass-shaped samples.

to be developed is the strain-induced crystallisation. Tests are conducted up to different strains in the range of 0–1.8 that are representative of the different steps of the deformation. Then, samples are quenched and thin slices are cut from specimens to be analysed using X-ray diffraction technique.

### 3.3. Quenching protocols

Taking into account the above considerations concerning quenching and annealing, a precise experimental protocol has to be defined involving cooling that is as rapid and as controlled as possible. As perfect quenching of massive samples is almost impossible, two methods, being referred to as bad and good quenching, are compared.

Bad quenching consists of stopping the test, opening the ambience chamber, removing the sample from the clamping devices and dropping it into cold water (0°C). It takes almost 30 s for the sample to be removed, during which the material is maintained at high temperature. Half of this duration corresponds to that of a constant length annealing (opening of the first grip). Then, annealing occurs free of constraint during the removal of the second grip before quenching. Finally, the sample is more or less quenched into the water free of constraint.

Good quenching consists of stopping the test, opening the ambience chamber and spraying cold water on 3/4 (due to accessibility) of the circumference of the sample to cool it keeping its length constant. The period of time during which the material is not cooled (opening of the chamber) remains lower than 3 s.

### 3.4. X-ray analysis

Analysis of the development of crystallinity could be done through the evolution of density or of DSC traces as in the literature. Nevertheless, these are indirect measure-

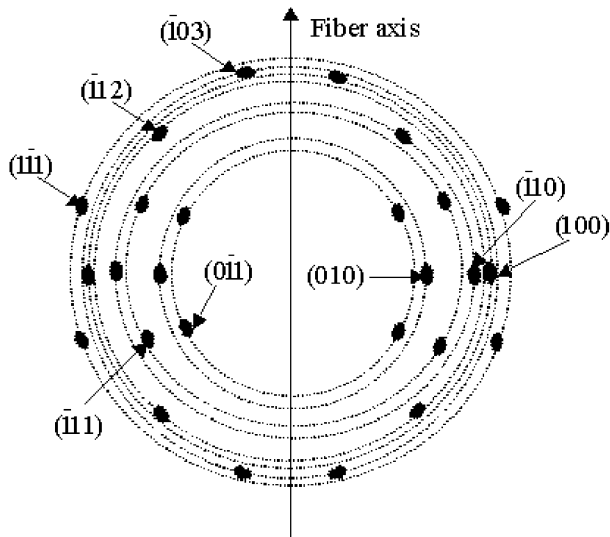


Fig. 3. Schematic X-ray diffraction pattern for a fibre texture of PET [17].

ments for crystallisation as density can vary even in an amorphous material (e.g. as a function of packing and orientation) and as the heating during DSC analysis could modify microstructure. For these reasons, we choose to use X-ray diffraction technique, which is mainly sensitive to actual ordered phases. In return, quantitative analysis remains difficult, especially in the case of oriented triclinic crystals as PET is, and will not be performed in this context.

In consequence, 300  $\mu\text{m}$ -thick slices are extracted from tensile specimens by polishing the zone where the strain was measured and where the strain-rate and the temperature were controlled. In the case of good quenching, the sample is cautiously cut from a zone as close as possible to the cooled part of the surface. Conversely, badly quenched samples are extracted in an axial section.

Transmission wide-angle X-ray diffraction experiments, using the flat-film camera technique (filtered  $\text{CuK}\alpha$  radiation) are performed on each sample. The Daubeny et al. [40] parameters (namely triclinic unit cell with  $a = 4.56 \text{ \AA}$ ,  $b = 5.94 \text{ \AA}$ ,  $c = 10.75 \text{ \AA}$ ,  $\alpha = 98.5^\circ$ ,  $\beta = 118^\circ$  and  $\gamma = 112^\circ$ ) are used to index the reflections. Patterns are qualitatively analysed in terms of perfection of crystalline phase and closeness to a fibre texture as reported by Gupte et al. [17] (Fig. 3). Due to our experimental conditions, we could not use the reflection associated to  $(\bar{1}05)$  planes which are almost perpendicular ( $10^\circ$  angle) [9] to chain axis. Nevertheless, most of the other reflections and, in particular, the very close  $(\bar{1}03)$  reflection can be observed and unambiguously indexed.

## 4. Results

The most complete observations are made during tensile tests at  $85^\circ\text{C}$  and  $0.01 \text{ s}^{-1}$  and are developed below. These results can be qualitatively extrapolated to other conditions provided that PET remains in its rubber-like state. It is verified that tensile tests are reproducible and that all the stress vs strain curves can be merged into an average one (Fig. 4). The different intermediate strain states studied intend to analyse PET as strain hardening is initiated and develops.

Whatever the quenching conditions are, low strain does not induce significant modification in the microstructure of the PET as revealed by the technique we use. Material remains unchanged, i.e. amorphous and isotropic, (Fig. 5A) up to the moment when a minimum value of the strain of almost 0.9 has been reached (Figs. 5B–D and 6A–D).

This value corresponds to the beginning of the mechanical strain hardening of the PET (Fig. 4). Then, simultaneously to further increases in the strain, the microstructure progressively changes (Figs. 5 and 6A–D) from an isotropic amorphous PET to a typical fibre texture parallel to the tensile direction (compare Figs. 3, 5D, 6D and 7), whereas strain hardening takes place and develops (Fig. 4). In a qualitative way, the changes in the

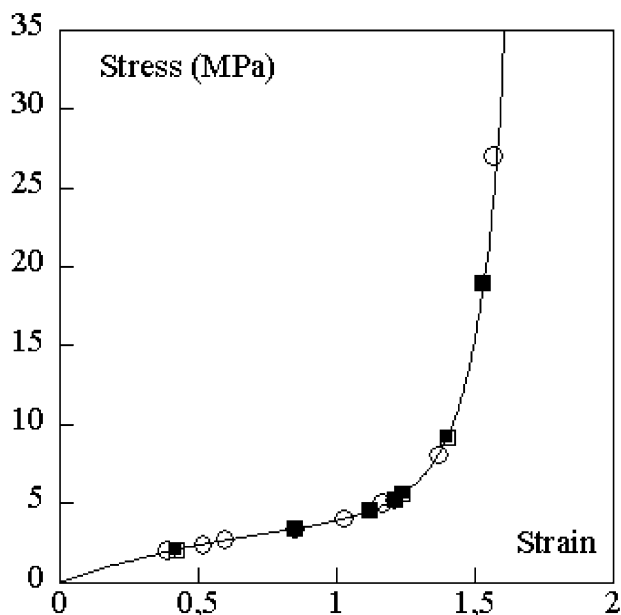


Fig. 4. Stress vs strain curve for a PET during tensile tests:  $0.01 \text{ s}^{-1}$  strain-rate and  $85^\circ\text{C}$ ; Definition of the intermediate strain levels analysed for a bad (■) or a good quenching (○) protocol.

microstructure are equivalent for both the two quenching protocols. Nevertheless, one can notice that a good quenching delays crystallisation and possibly avoids some small tilting of specific reflections (Figs. 5 and 6), being the final textures at high strain equivalent.

First evidence for an ordered phase are the (010) and (100) equatorial reflections corresponding to Daubeny parameters, but being characteristic for small in comparison to classical lamellae thickness for PET (3.8–4.8 nm [10,25]) or imperfect crystals as suggested by the spreading out of the diffraction spots. The location of these spots demonstrates a significant amount of orientation of the chains axis parallel to the tensile direction even at the very first stages of the development of the microstructure. Conversely, ( $\bar{1}03$ ) reflection cannot be observed, suggesting these first stages could result from the nucleation of a kind of micelle-like imperfect crystal (or mesophase) parallel to the tensile axis and organised at a spatial scale equivalent to final crystal throughout a section, but with no ‘vertical’ organisation (i.e. along *c*-axis) or with an organisation at a scale different from that of the final crystal (i.e. not visible in our experiments).

Three additional differences between the considered quenching protocols have to be emphasised:

- the evolution as a function of strain is much faster in the case of bad quenching (Fig. 5) than in the case of good quenching (Fig. 6) for which crystallisation seems to be less perfect,
- equatorial reflections (010) and (100) are tilted in the case of badly quenched samples in an equivalent manner to what was reported after annealing low oriented fibres

[17,18] or films [22,41,42], whereas well quenched samples exhibited a microstructure less sensitive to annealing [43],

- abnormal meridian (010) and (100) reflections are also observed in badly quenched samples being a trace of a possible orthogonal bi-orientation of molecules, which cannot be explained by the imposed loading.

The first of these remarks suggests that part of the ‘crystallisation’ could occur after deformation, during cooling which acts as an annealing process allowing a partial of relaxation of molecular orientation leading to the second of these observations. Third point, for its part, could be a trace of annealing or a trace of orientation initiation due to the flow pattern during injection moulding of the samples. Identical diffraction can be found even in the case of good quenching when sample is extracted far from the sprayed surface (Fig. 8), i.e. in a location where quenching is less efficient.

Once a drastic strain hardening process has begun, the first trace for a longitudinal order appears. Firstly, ( $\bar{1}03$ ) reflection (Figs. 5C and 6C) becomes visible followed by ( $\bar{1}12$ ) reflection (Fig. 5D)). In parallel, tilts and abnormal reflections disappear (Figs. 5C and 6C) while other reflections increase in intensity and definition remaining at the same locations. At high strain (1.4 or 1.8 depending on quenching protocols) a ‘perfect’ fibre texture is observed being no more sensitive to the quality of the cooling process. Following these observations, first observable stages for crystallisation could be oriented to small micelle-like imperfect crystals whose perfection increases as strain increases.

## 5. Discussion and conclusion

The results presented here together with recent literature [29–33] enable us to conclude that, even if strain hardening in PET can be correlated to crystallisation, the kinetics of appearance of crystals and their effect on the behaviour of the polymer are not totally clear.

Due to the drastic increase in crystallisation kinetics induced by molecular extension, it is almost impossible to set the microstructure of an oriented PET. The latter could always crystallise during quenching. In addition, such deformed PET can remain highly oriented after annealing. That is, when oriented PET crystallises, crystallisation is so rapid that orientation can be trapped and that induced texture is still controlled by previous loading conditions. Consequently, final crystallinity ratio measured after deformation and cooling should strongly depend on the cooling applied to the material after deformation. On the contrary, final orientation of the crystal should mainly depend on the deformation.

Our results demonstrate that it is possible to obtain a non-fully semi-crystalline polymer under strain even after strain hardening has been initiated (Fig. 6). As a matter of

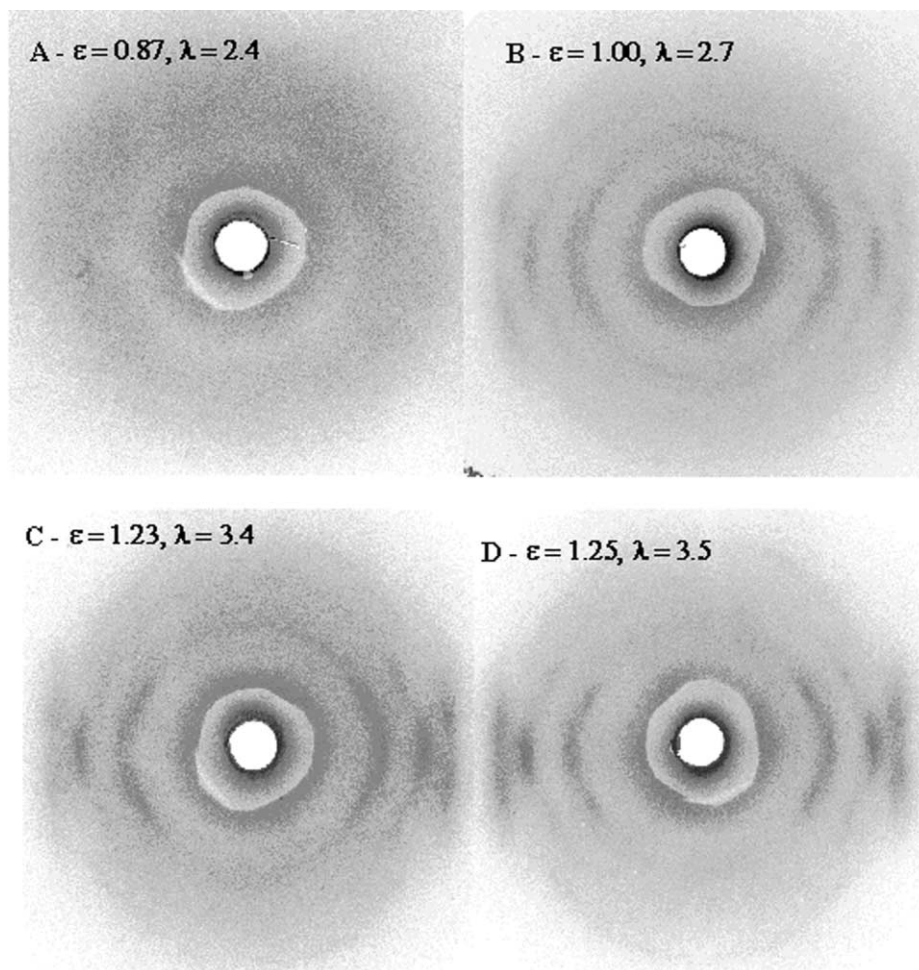


Fig. 5. Typical X-ray diffraction patterns for badly quenched samples as a function of the strain ( $\epsilon$ ) or the draw ratio ( $\lambda$ ). Tensile axis is always parallel to the vertical direction.

fact, first steps of crystallisation result from the appearance of small zones having the lateral order of the crystal and being oriented parallel to the tensile direction. Longitudinal order appears later on to progressively lead to a perfect fibre-texture. Before the crystalline texture has been totally developed during the deformation (i.e. at low strain) the cooling kinetics strongly influence the observed microstructure by superposing secondary steps in the crystallisation in which crystallisation of oriented molecules and orientation relaxation can compete.

Summarising our results and recent literature [29,33], a possible scheme for microstructure formation in PET under strain can be proposed (Fig. 9). Firstly, deformation orients molecules reinforcing or promoting interaction between them. These interactions lead the appearance of ordered entities, or precursors, which are oriented, as a result to molecular orientation. They can be the suggested smectic phase [33] or a mesophase, but they are not a fully developed crystalline phase. These zones act as crosslinks. In the first step (orientation stage in Fig. 9), these entities are neither numerous nor tightened enough to promote either strain hardening or significant crystallisation during cooling

or deformation. At a given level of strain, the number of these entities is such that the strain hardening of the resulting network is significant (nucleation stage in Fig. 9). Actual crystallisation, for its part, necessitates a certain accommodation time or a minimum level of molecular relaxation to be effective. So, in that region crystallisation should occur during cooling if the deformation is stopped, as a result of a competition between molecular relaxation and crystal growth. Then, accurately quenched samples exhibit non-perfect crystals more or less close to the precursors depending on the deformation duration or/and the cooling rate. In the following stage (growth stage in Fig. 9), one can imagine that either existing entities have time to grow under deformation or crystallisation kinetics is so rapid (due to orientation) during cooling that true crystals can be observed.

If this scheme is correct, depending on strain-rate, crystallisation may or may not occur during deformation. Consequently, at high strain-rate, the material should remain quasi amorphous after deformation as observed using synchrotron beams [29,30] before cooling. This analysis can explain the apparent contradiction between

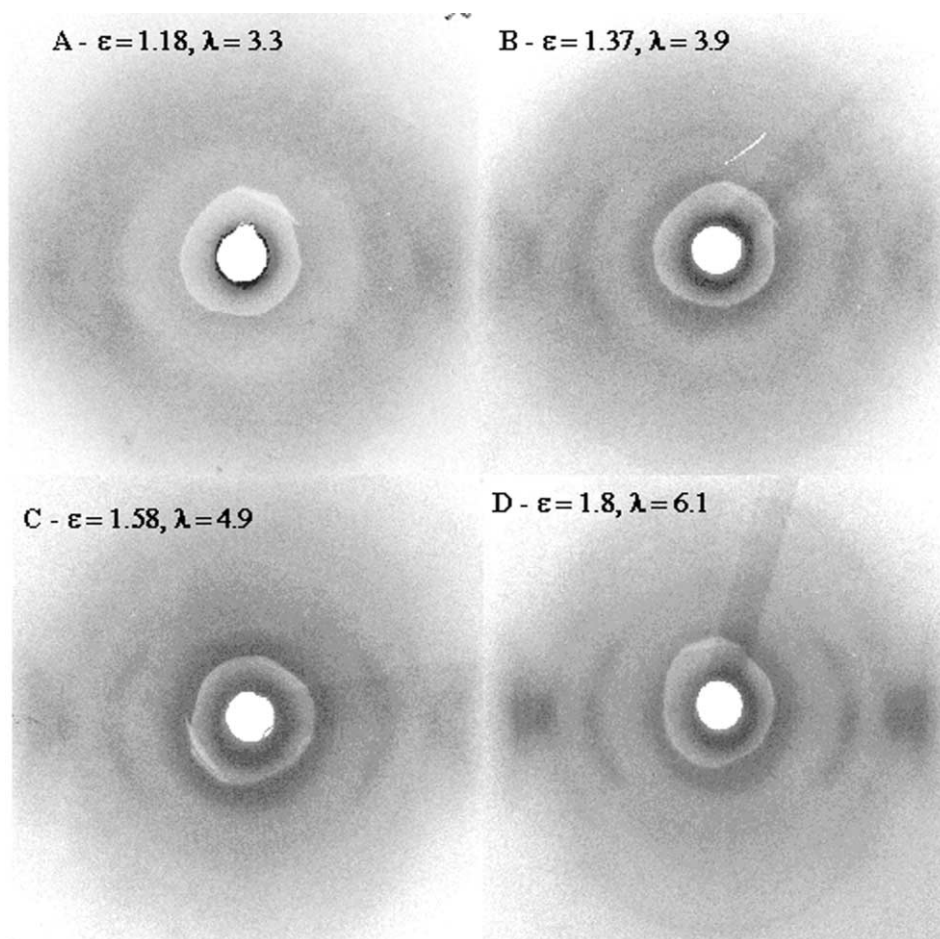


Fig. 6. Typical X-ray diffraction pattern for well-quenched sample as a function of the strain ( $\epsilon$ ) or the draw ratio ( $\lambda$ ). Tensile axis is always parallel to the vertical direction.

well-known results concerning the correlation between crystallinity ratio and strain and in-situ measurements.

Another point to be considered is the fact that the PET used in this study has been modified to slow down the crystallisation, as said before, whereas previous study

could use different resin. Unambiguous comparison between all these results should require a better description of all the polymers.

However, our experiments clearly show that there is no direct relationship between crystallinity and strain hardening.

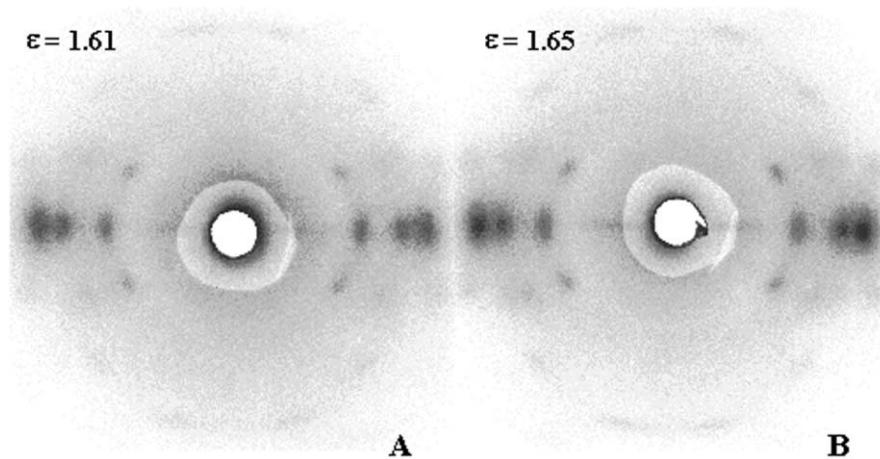


Fig. 7. X-ray diffraction patterns for a samples deformed at 95°C and for a constant cross-head velocity of 25 mm s<sup>-1</sup> (initial strain rate of 2 s<sup>-1</sup>). Comparison between a bad quenching (A) and a good quenching (B). Tensile axis is always parallel to the vertical direction.

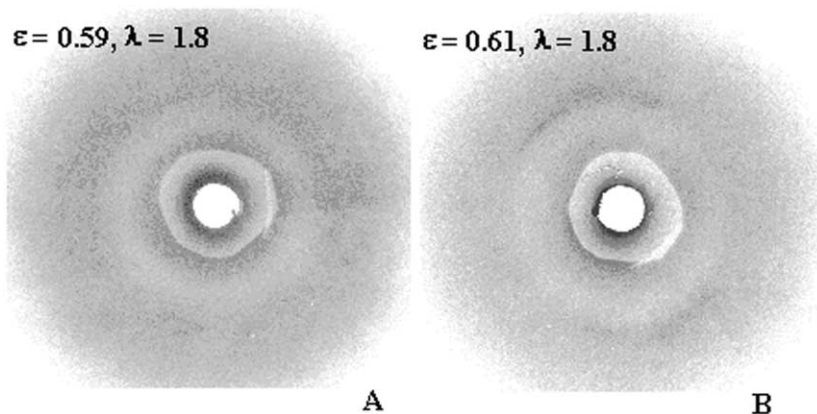


Fig. 8. X-ray diffraction patterns for a samples deformed at 85°C and strain rate of 0.01 s<sup>-1</sup> and quenched according to the good quenching protocol. Comparison between a sample extracted close to the quenching zone (A) and an axial section (B). Tensile axis is always parallel to the vertical direction.

The relationships to be established should relate strain hardening to nucleation as crystallinity ratio depends on both strain and cooling.

As a consequence, crystallinity ratio is not the accurate parameter to be introduced in models for a constitutive equation for PET even if, in certain case [44], some sets of experiments enable to draw empirical relationships between these two parameters. Obviously, at the laboratory level, once external cooling conditions have been defined, there can exist a relation between nucleation under strain and crystallisation during cooling, but results cannot be extrapolated to other situations without a high level of risk.

Additional experiments should be necessary to confirm our assumptions. However, from an experimental point of view, our results unambiguously prove that ordered phase in PET could be a non-fully formed crystal even once strain hardening has been promoted. This enlightens the fact that strain hardening is due to interaction between chains, e.g.

nucleation leading to some kind of crosslinks, but does not necessitate perfect and large crystals.

### Acknowledgements

This work was sponsored by Tergal-Fibres (Rue Jules Vercausse, BP 1, 02430 Gauchy, France) and Sidel (Av. de la Patrouille de France, Octeville-sur-Mer, BP 204, 76053 Le Havre Cedex, France) companies.

The authors thank G. Pérez, D. Darras and J.L. Lepage for financial and technical support and G. Monge for his help on X-ray diffraction technique.

### References

- [1] Ward IM. *Adv Polym Sci* 1985;66:81–115.
- [2] Faisant de Champchesnel JB, Bower DI, Ward IM, Tassin JF, Lorentz G. *Polymer* 1993;34(18):3763–70.
- [3] Lapersonne P, Tassin JF, Monnerie L. *Polymer* 1994;35(10):2192–6.
- [4] Bower DI, Jarvis DA, Ward IM. *J Polym Sci Polym Phys Ed* 1986;24(7):1459–80.
- [5] Jarvis DA, Hutchinson IJ, Bower DI, Ward IM. *Polymer* 1980;21(1):41–54.
- [6] Lapersonne P, Bower DI, Ward IM. *Polymer* 1992;33(6):1277–83.
- [7] Dargent E. PhD Thesis, Université de Rouen, France, 1994.
- [8] Aji A, Guèvremont J, Cole KC, Dumoulin MM. *Polymer* 1996;37(16):3707–14.
- [9] Lapersonne P. PhD Thesis, Université de Paris VI, France, 1991.
- [10] Lapersonne P, Tassin JF, Monnerie L, Beutemps J. *Polymer* 1991;32(18):3331–9.
- [11] Aji A, Cole KC, Dumoulin MM, Brisson J. *Polymer* 1995;36(21):4023–30.
- [12] Pearce R, Cole KC, Aji A, Dumoulin MM. *Polym Engng Sci* 1997;37(11):1795–800.
- [13] Le Bouvellec G, Beutemps J. *J Appl Polym Sci* 1990;39(2):319–28.
- [14] Le Bouvellec G, Monnerie L, Jarry JP. *Polymer* 1986;27(6):856–60.
- [15] Salem DR. *Polymer* 1992;33(15):3182–8.
- [16] Salem DR. *Polymer* 1992;33(15):3189–92.
- [17] Gupte KM, Motz H, Schultz JM. *J Polym Sci Polym Phys Ed* 1983;21(10):1927–53.
- [18] Pezkin PN, Schultz JM. *J Polym Sci Part B: Polym Phys* 1986;24(12):2591–616.

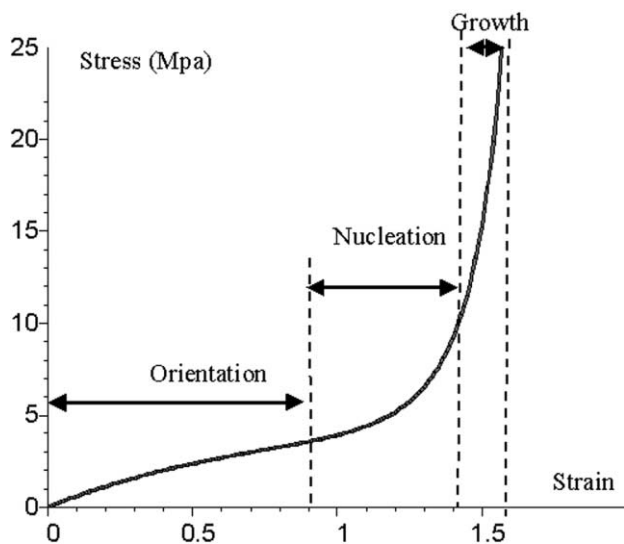


Fig. 9. Schematic kinetics of microstructure development in PET.



- [19] Lee KG, Schultz JM. *Polymer* 1993;34(21):4455–70.
- [20] Misra A, Stein RS. *J Polym Sci Polym Phys Ed* 1979;17(2):235–57.
- [21] Jabarin SA. *Polym Engng Sci* 1984;24(5):376–84.
- [22] Cakmak M, Spruiell JE, White JL, Lin JS. *Polym Engng Sci* 1987;27(12):893–905.
- [23] Hoffmann D, Göschel U, Walenta E, Geiss D, Philipp B. *Polymer* 1989;30(2):242–7.
- [24] Lapersonne P, Faisant de Champchesnel JB, Lorentz G, Tassin JF, Monnerie L, Bower DI, Ward IM. Proceedings of the Ninth Annual Meeting of the Polymer Processing Society, Manchester, UK, 1993, PPS-9. p. 99–100.
- [25] Göschel U, Urban G. *Polymer* 1995;36(19):3633–9.
- [26] Jabarin SA. *Polym Engng Sci* 1992;32(18):1341–9.
- [27] Greener J, Tsou AH, Blanton TN. Proceedings of SPE RETEC International Symposium On Orientation of Polymers; Application to Films and Fibers, Orientation of Polymers, Boucherville, Canada, 1998. p. 39–93.
- [28] Wilson MPW. *Polymer* 1974;15(2):277–82.
- [29] Ryan AJ. Proceedings of the 11th Annual Meeting of the Polymer Processing Society, Seoul, Korea, 1995, PPS-11. p. 331–2.
- [30] Blundell DJ, Mac Kerron DH, Fuller W, Mahendrasingam A, Martin C, Oldman RJ, Rule RJ, Riekel C. *Polymer* 1996;37(15):3303–11.
- [31] Welsh GE, Blundell DJ, Windle AH. *Macromolecules* 1998;31(21):7562–5.
- [32] Asano T, Balta Calleja FJ, Flores A, Tanigaki M, Forhad Mina M, Sawatari C, Itagaki H, Takahashi H, Hatta I. *Polymer* 1999;40(23):6475–84.
- [33] Mahendrasingam A, Martin C, Fuller W, Blundell DJ, Oldman RJ, Mac Kerron DH, Harvie JL, Riekel C. *Polymer* 2000;41(3):1217–21.
- [34] Patkar M, Jabarin SA. *J Appl Polym Sci* 1993;47(10):1749–63.
- [35] Di Fiore C, Leone B, De Rosa C, Guerra G, Petraccone V, Di Dino G, Bianchi R, Vosa R. *J Appl Polym Sci* 1993;48(11):1997–2001.
- [36] G'Sell C, Hiver JM, Dahoun A, Souahi A. *J Mater Sci* 1992;27:5031–9.
- [37] Gorlier E, Agassant JF, Haudin JM, Billon N. Proceedings of the International Workshop on Video-controlled Materials Testing and In-situ Microstructural Characterization, Nancy, France, 1999. p. 28.
- [38] Gorlier E, Agassant JF, Haudin JM, Billon N. Proceedings of the 11th International Conference On Deformation Yield and Fracture of Polymers, Cambridge, UK, 2000. p. 351–4.
- [39] Gorlier E, Agassant JF, Haudin JM, Billon N. *Plastics. Rubber and Composites* 2001;30(2):48–55.
- [40] Daubeny RP, Bunn CW, Brown CJ. *Proc R Soc Lond* 1954;A(226):531–42.
- [41] Biangardi HJ, Zachmann HG. *J Polym Sci Polym Symp* 1977;58:169–83.
- [42] Stockfleth J, Salamon L, Hinrichsen G. *Colloid Polym Sci* 1993;271(5):423–35.
- [43] Casey M. *Polymer* 1977;18(12):1219–26.
- [44] G'Sell C, Hiver JM, Elkoun S, Vigny M, Cabot C, Aubert A, Dahoun A. Proceedings of the 11th International Conference On Deformation Yield and Fracture of Polymers, Cambridge, UK 2000. p. 375–8.